

## Preparation and luminescence of $\text{Sr}_3\text{MgSi}_2\text{O}_8 : \text{Eu}^{2+}$ blue-emitting phosphors

Jaehan Park and Young Jin Kim\*

Department of Materials Science and Engineering, Kyonggi University, Suwon 443-760, Korea

$\text{Sr}_3\text{MgSi}_2\text{O}_8 : \text{Eu}^{2+}$  blue-emitting phosphors were prepared by a flux method and their luminescent properties were investigated. The excitation spectra were broad (250–500 nm), showing strong excitation intensities at 370–410 nm, while the intense blue emission was observed at around 460 nm assigned to the  $4f^65d^1-4f^7$  transition of the  $\text{Eu}^{2+}$  ions incorporated into the Sr(I) sites. The strongest emission was obtained from the starting mixture with the excess Sr content. The emission intensity varied with firing temperatures, an amount of a flux, and the Eu content. These luminescent properties demonstrate that  $\text{Sr}_3\text{MgSi}_2\text{O}_8 : \text{Eu}^{2+}$  powders are promising blue phosphors for use in white light emitting diodes using near ultraviolet chips.

**Key words:** Strontium magnesium silicate, Phosphor, Luminescence.

### Introduction

White light-emitting diodes (WLEDs), which are composed of LED chips and phosphors, have been extensively developed for use in solid-state lightings. There are two alternative ways of making WLEDs, which combine blue or near ultraviolet (nUV) LED chips with a phosphor blend. The latter has some advantages over the former in color rendering index, color temperature, chip performance, etc.

For WLEDs using nUV chips, multi-emitting phosphor blends (red, green, and blue) are required to generate white light, while a blue-emitting phosphor is very important because of its small Stokes shift and critical contribution to white light generation [1]. Some of the most efficient blue-emitting phosphors are  $\text{Eu}^{2+}$  doped halo-phosphates [2] and silicate compounds including  $\text{X}_3\text{MgSi}_2\text{O}_8$  (X:  $\text{Sr}^{2+}$ ,  $\text{Ca}^{2+}$ , and  $\text{Ba}^{2+}$ ) [3–12].  $\text{Sr}_3\text{MgSi}_2\text{O}_8$  (SMSO) has a monoclinic structure, and its space group (P12<sub>1</sub>/c1) corresponds to that of merwinite ( $\text{Ca}_3\text{MgSi}_2\text{O}_8$ ) [12]. There are three different Sr sites: 12-coordinated Sr(I); 10-coordinated Sr(II) and Sr(III) [12, 13].  $\text{Eu}^{2+}$  doped SMSO (SMSO :  $\text{Eu}^{2+}$ ) has a broad photoluminescence excitation (PLE) spectrum, covering up to ~ 500 nm and exhibits a strong blue emission band at around 455 nm [3–5]. SMSO co-doped with  $\text{Mn}^{2+}$  and  $\text{Eu}^{2+}$  was reported to generate blue and red light simultaneously [7–8]. However, despite the excellent emission properties of SMSO :  $\text{Eu}^{2+}$ , the systematic investigation of the effects of preparation parameters on the luminescence has rarely been reported.

In this study, SMSO :  $\text{Eu}^{2+}$  powders were prepared by a

flux method. The effects of preparation conditions including firing temperatures, an amount of a flux, the Eu concentration, and the composition of the starting mixture on the structure and the emission were systematically investigated.

### Experiment

SMSO :  $\text{Eu}^{2+}$  powders were prepared by firing the mixtures of  $x\text{SrCO}_3\text{-MgCO}_3\text{-}2\text{SiO}_2\text{-}y/2\text{Eu}_2\text{O}_3$  using a conventional solid-state reaction method.  $\text{SrCO}_3$  (Aldrich, 99.9%),  $\text{SiO}_2$  (High purity chemical, 99.9%),  $\text{Eu}_2\text{O}_3$  (Aldrich, 99.99%),  $\text{MgCO}_3$  (High purity chemical, 99.9%+), and  $\text{NH}_4\text{Cl}$  (Aldrich, 99.99%) were used as starting materials. The mixed powders were fired at 1200–1500 °C for 3 hrs in an electric tube furnace under 5%  $\text{H}_2$  (95%  $\text{N}_2$ ) atmosphere. The crystalline phase was determined by an X-ray diffractometer (XRD, Rigaku Miniflex2) using  $\text{Cu}_{K\alpha}$  radiation ( $\lambda = 1.5406 \text{ \AA}$ ). The particle morphology was analyzed by a field emission scanning electron microscope (FE-SEM, Hitachi S-4800). The crystal parameters were estimated by X'pert HighScore Plus of PANalytical B. V. The photoluminescence (PL) was measured using a PL system (PSI, Darsa 5000) with a 500 W xenon lamp as an excitation source at room temperature.

### Results and Discussion

The XRD patterns of the samples prepared with various  $x$  values of the starting mixtures of  $x\text{SrCO}_3\text{-MgCO}_3\text{-}2\text{SiO}_2\text{-}0.01\text{Eu}_2\text{O}_3$  at 1300 °C are shown in Fig. 1. The XRD patterns at  $x = 3.0$  corresponded to those of ICSD #17-3780 [12], indicating that SMSO was produced as a dominant phase, while the  $\text{Sr}_2\text{MgSi}_2\text{O}_7$  phase weakly coexisted. The  $\text{Sr}_2\text{MgSi}_2\text{O}_7$  phase became negligible at  $x = 3.05$  and above, whereas the  $\alpha'$ -

\*Corresponding author:  
Tel : +82-31-249-9766  
Fax : +82-31-244-6300  
E-mail: yjkim@kyonggi.ac.kr

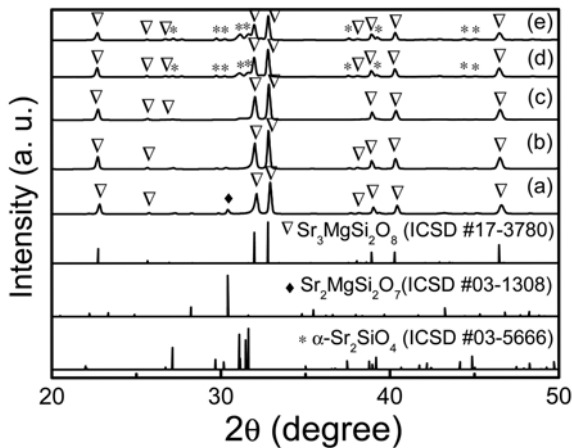


**Fig. 1.** XRD patterns of the samples prepared with the starting mixture of  $x\text{SrCO}_3\text{-MgCO}_3\text{-2SiO}_2\text{-0.01Eu}_2\text{O}_3$ . (a)  $x = 3.0$ , (b)  $x = 3.05$ , (c)  $x = 3.1$ , (d)  $x = 3.2$ , and (e)  $x = 3.3$ .

**Table 1.** Crystal parameters of  $\text{Sr}_3\text{MgSi}_2\text{O}_8$  prepared at  $x = 3.05$ . [Unit: Å, degree]

Sample	a	b	c	$\alpha$	$\beta$	$\gamma$	unit cell volume
Reference	9.4520	5.4580	13.8770	90	90	90	715.90 Å <sup>3</sup>
This work	9.4246	5.4704	13.8810	90	89.6	90	715.27 Å <sup>3</sup>

$\text{Sr}_2\text{SiO}_4$  ( $\alpha'$ -SSO) phase appeared at more than  $x = 3.2$ . The crystal parameters ( $x = 3.05$ ) are given in Table 1, indicating that they are nearly the same as the reference data, ICSD #17-3780 [12].

Corresponding PL excitation (PLE) and PL spectra are exhibited in Fig. 2. The PLE spectra (left) are broad and show the strong intensities at around 350-410 nm, while the red-shift was observed with increasing  $x$  values except  $x = 3.3$ . This result demonstrates that  $\text{SMSO}:\text{Eu}^{2+}$  powders are very suitable for WLEDs using uUV LED chips. The strong emission bands were observed at around 457 nm, depending on the amount of  $\text{SrCO}_3$  ( $x$ ). This luminescence originated from the  $4f^7\text{-}4f^65d^1$  transition of the  $\text{Eu}^{2+}$  ions that were incorporated into the  $\text{Sr}^{2+}$  sites. It is highly probable

that the  $\text{Eu}^{2+}$  ion is substituted for the  $\text{Sr}^{2+}$  ion, because its ionic radius (1.17 Å, coordination number (CN) = 6) is nearly the same as that of  $\text{Sr}^{2+}$  (1.18 Å), whereas those of  $\text{Mg}^{2+}$  (0.72 Å) and  $\text{Si}^{4+}$  (0.4 Å) are too small to allow the  $\text{Eu}^{2+}$  substitution. The emission spectra (right) exhibit strong blue emissions at around 460 nm. As described above, there are three Sr sites, accordingly the  $\text{Eu}^{2+}$  ions can be substituted for each Sr site, resulting in the Eu(I), Eu(II), and Eu(III) sites. It was reported that the emission spectrum of  $\text{SMSO}:\text{Eu}^{2+}$  consisted of a strong peak at 470 nm due to Eu(I) and a weak peak at 570 nm due to Eu(II) and Eu(III) [7-8]. However, in Fig. 2 (right), the 570 nm emissions were negligible at  $x = 3.0\text{-}3.1$ , whereas they were apparent at  $x = 3.2\text{-}3.3$ . The blue emission intensity gradually increased up to  $x = 3.2$  and abruptly decreased at  $x = 3.3$ , while a slight red-shift of the dominant peak wavelength (DPW) was observed at  $x = 3.2\text{-}3.3$ , as shown in the inset of Fig. 2. The presence of the  $\alpha'$ -SSO impurity phase at  $x = 3.2\text{-}3.3$  probably contributed to the emission properties in two ways. First, the emission spectra of  $\alpha'$ -SSO: $\text{Eu}^{2+}$  are composed of two emission bands at about 495 and 560 nm [14]. Accordingly, it is unclear whether the weak 570 nm emissions in Fig. 2 originated from Eu(II) and Eu(III) of  $\text{SMSO}:\text{Eu}^{2+}$  and/or Eu(II) of  $\alpha'$ -SSO: $\text{Eu}^{2+}$ . Another way is to share the Eu content, because the  $\text{Eu}^{2+}$  ions can be incorporated into  $\alpha'$ -SSO as well as SMSO. Therefore, the presence of  $\alpha'$ -SSO might reduce the Eu content in SMSO, leading to the optimum Eu concentration for the strongest emission of  $\text{SMSO}:\text{Eu}^{2+}$ . The abrupt decrease in the emission intensity at  $x = 3.3$  can not be explained at this stage.

The dependence of the emission intensity on the firing temperature is shown in Fig. 3 (left). The change in the XRD patterns with the firing temperature was insignificant at 1200-1400 °C, but the  $\text{Sr}_2\text{MgSi}_2\text{O}_7$  phase apparently appeared as an impurity phase at 1500 °C. At 1200-1400 °C, the emission intensity continuously increased, because the increase in the firing temperature caused the enhancement of the crystallinity and

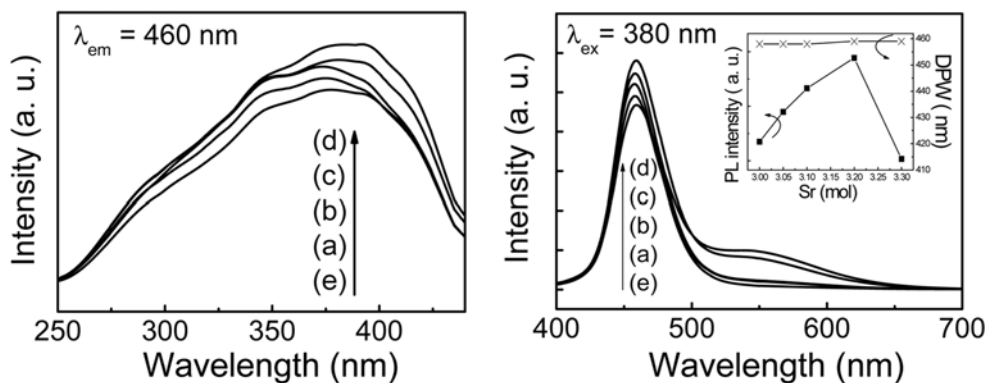


**Fig. 2.** PLE (left) and PL (right) spectra of the samples prepared with the starting mixture of  $x\text{SrCO}_3\text{-MgCO}_3\text{-2SiO}_2\text{-0.01Eu}_2\text{O}_3$ . (a)  $x = 3.0$ , (b)  $x = 3.05$ , (c)  $x = 3.1$ , (d)  $x = 3.2$ , and (e)  $x = 3.3$ .

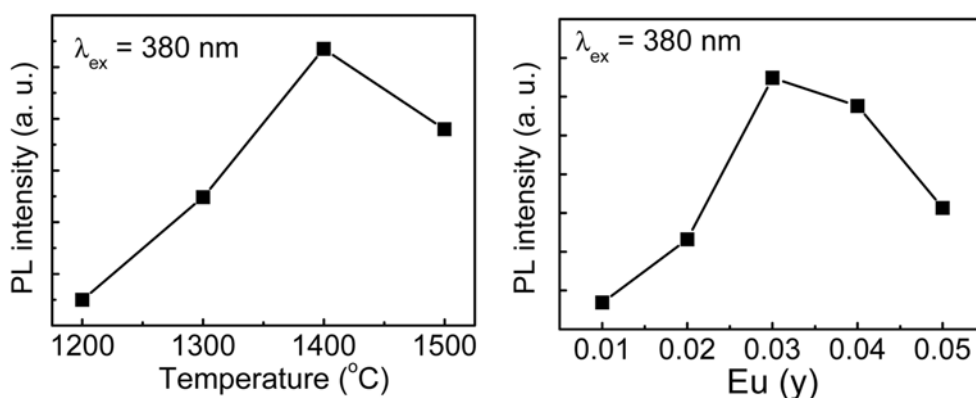


Fig. 3. Variation of the emission intensity with different firing temperatures (left) and Eu contents ( $y$ ) (right).

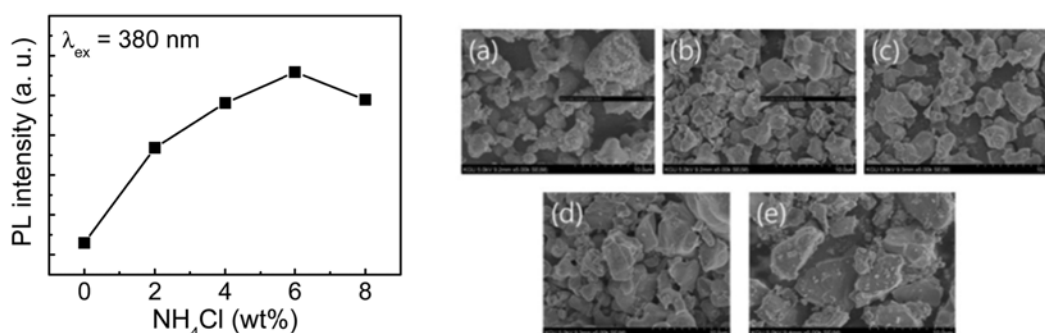


Fig. 4. Variation of the emission intensity (left) and SEM micrographs of the synthesized powders (right) with different amounts of a flux ( $\text{NH}_4\text{Cl}$ ). (a) 0 wt%, (b) 2 wt%, (c) 4 wt%, (d) 6 wt%, and (e) 8 wt%.

reduced the micro defects included in the particles. The presence of  $\text{Sr}_2\text{MgSi}_2\text{O}_7 : \text{Eu}^{2+}$  resulted in the drop of the emission intensity at 1500 °C and the slight red-shift of DPW [4].

The variation of the emission intensity as a function of the Eu content ( $y$ ) is shown in Fig. 3 (right); the emission intensity peaked at  $y = 0.03$  and decreased at more than  $y = 0.04$  due to the concentration quenching effect. The average distance ( $R_{\text{avg}}$ ) of  $\text{Eu}^{2+}$ - $\text{Eu}^{2+}$  is shortened with the increase in the Eu concentration, and it becomes shorter than the critical distance of the energy transfer ( $R_c$ ), resulting in the decrease in the emission intensity above the optimum Eu concentration [14]. With the Eu concentration, the change in DPW was insignificant in this study, whereas the earlier work [4] reported that DPW moved toward longer wavelengths.

The effects of an amount of the flux ( $\text{NH}_4\text{Cl}$ ) were investigated and the change in the emission intensity (left) and the particle morphology (right) are shown in Fig. 4. The strongest emission intensity was observed at 6 wt%  $\text{NH}_4\text{Cl}$ . The addition of the flux facilitated the incorporation of the  $\text{Eu}^{2+}$  ions into SMSO, accordingly enhanced the emission intensity. On the other hand, at 8 wt%  $\text{NH}_4\text{Cl}$ , the emission intensity decreased because of enlarged particle size as shown in Fig. 4.

### Conclusions

SMSO: $\text{Eu}^{2+}$  powders were prepared by firing the

mixtures of  $x\text{SrCO}_3$ - $\text{MgCO}_3$ - $2\text{SiO}_2$ - $y/2\text{Eu}_2\text{O}_3$ . The excitation spectra were broad and peaked at around 380 nm, and the strong blue emission band was achieved at around 460 nm that originated from the firing temperatures, an amount of a flux, and the Eu content, while the strongest emission was obtained at 1400 °C, 6 wt%  $\text{NH}_4\text{Cl}$ , and 0.03 mole Eu. These findings indicated that SMSO :  $\text{Eu}^{2+}$  powders are promising blue phosphors for use in WLEDs pumped by nUV sources.

### Acknowledgments

This work was supported by the National Research Foundation of Korea (NRF) grant funded by the Korea government (MEST) (NRF-2011-0013554) and Kyonggi University's Graduate Research Assistantship 2013. Thanks to Mr. Daniel Lee at PANalytical for XRD analysis.

### References

1. J. McKittrick, M.E. Hannah, A. Piquette, J.K. Han, J.I. Choi, M. Anc, M. Galvez, H. Lugauer, J.B. Talbot, and K.C. Mishra, *ECS J. Solid State Sci. Technol.* 2 (2013) R3119-R3131.
2. M.H. Hwang, E.Y. Lee, S.-H. Hong, Y.-B. Sun, and Y.J. Kim, *J. Electrochem. Soc.* 156 (2009) J185-J188.
3. S. Hwangbo, Y.-S. Jeon, B.-A. Kang, Y.-S. Kim, K.-S. Hwang, and J.-T. Kim, *J. Ceram. Process. Res.* 11 (2010) 513-515.

4. J.K. Park, K.J. Choi, C.H. Kim, H. D. Park, and H. K. Kim, *Electrochem. Solid State Lett.* 7 (2004) H42-H43.
5. T.L. Barry, *J. Electrochem. Soc.* 115 (1968) 733-738.
6. H.-K. Jung and K.S. Seo, *Opt. Mater.* 28 (2006) 602-605.
7. J.S. Kim, P.E. Jeon, Y.H. Park, J.C. Choi, and H.L. Park, *Appl. Phys. Lett.* 85 (2004) 3696-3698.
8. J.S. Kim, P.E. Jeon, Y.H. Park, J.C. Choi, and H.L. Park, *J. Electrochem. Soc.* 152 (2005) H29-H32.
9. W. Pan and G. Ning, *Sens. Actuator A-Phys.* 139 (2007) 318-322.
10. Y. Umetsu, S. Okamoto, and H. Yamamoto, *J. Electrochem. Soc.* 155 (2008) J193-J197.
11. J.S. Kim, P.E. Jeon, J.C. Choi, and H.L. Park, *Appl. Phys. Lett.* 84 (2004) 2931-2933.
12. Y. Yonesaki, T. Takei, N. Kumada, and N. Kinomura, *J. Solid State Chem.* 182 (2009) 547-554.
13. P.B. Moore and T. Araki, *Am. Mineral.* 57 (1972) 1355-1374.
14. J.H. Lee and Y.J. Kim, *Mater. Sci. Eng. B* 146 (2008) 99-102.